Postprint of: Li X., Sadiq S., Zhang W., Chen Y., Xu X., Abbas A., Chen S., Zhang R., Xue G., Sobotka D., Makinia J., Salinity enhances high optically active L-lactate production from co-fermentation of food waste and waste activated sludge: Unveiling the response of microbial community shift and functional profiling, Bioresource Technology, Vol. 319 (2021), 124124, DOI: 10.1016/j.biortech.2020.124124

Salinity enhances high optically active L-lactate production from co-fermentation of food waste and waste activated sludge: Unveiling the response of microbial community shift and functional profiling

Xiang Li[a], Safeena Sadiq[a], Wenjuan Zhang[d], Yiren Chen[a], Xianbao Xu[a,*], Anees Abbas[f], Shanping Chen[e], Ruina Zhang[e], Gang Xue[a,c], Dominika Sobotka[b], Jacek Makinia[b]

[a] *State Environmental Protection Engineering Centre for Pollution Treatment and Control in Textile Industry, College of Environmental Science and Engineering, Donghua University, 2999 North Renmin Road, Shanghai 201620, China*

[b] *Faculty of Civil and Environmental Engineering, Gdansk University of Technology, ul. Narutowicza 11/12, 80-233 Gdansk, Poland*

[c] *Shanghai Institute of Pollution Control and Ecological Security, Shanghai 200092, China*

[d] *College of Chemistry and Chemical Engineering, Shanghai University of Engineering Science, Shanghai, 201620, China*

[e] *Shanghai Municipal Solid Waste Engineering Technology Research Center, Shanghai Institute for Design & Research on Environmental Engineering Co., Ltd, Shanghai Environmental Sanitary Engineering Design Institute Co., Ltd, Shilong Road 345, Shanghai, 200232, China*

[f] *Department of chemistry, University of Mianwali, 42200 Mianwali, Pakistan*

*Corresponding author

E-mail: 18621035295@163.com
Tel: 86-21-67792538

Fax: 86-21-67792159

Abstract

Lactic acid (LA), a versatile platform molecule, can be fermented from organic wastes, such as food waste and waste activated sludge. In this study, an efficient approach using salt, a component of food waste as an additive, was proposed to increase LA production. The LA productivity was increased at 10 g NaCl/L and optical pure L-lactate was obtained at 30 g NaCl/L. The enhancement of LA was in accordance with the increased solubilization and the critical hydrolase activities under saline conditions. Moreover, high salinity (30-50 g NaCl/L) changed the common conversion of LA to volatile fatty acids. In addition, the key LA bacteria genera (*Bacillus, Enterococcus, Lactobacillus*) were selectively enriched under saline conditions. Strong correlations between salinity and functional genes for L-LA production were also observed. This study provides a practical way for the enrichment of L-LA with high optical activity from organic wastes.

Keywords: Lactic acid, Optical activity, Salt, Food waste, Waste activated sludge

1. Introduction

Lactic acid (LA) is one of the most versatile platform molecules and widely used in food industries, medicine, and chemical industries (Pejin et al. 2018). Especially, poly-lactic acid (PLA), a promising biodegradable plastic, can be polymerized from LA. The physical properties of PLA, including heat resistance, are highly depended on L-lactic acid optical activity (OA-L) (Lunt 1998, Lv et al. 2019). The chemical synthesis of LA generates racemic mixture, whereas LA with high optical activity (OA) can be obtained by microbial fermentation (Zhang et al. 2017). Inoculation of specific lactic acid bacteria (LAB) could obtain optical pure isomer (Meng et al. 2012, Ye et al. 2013), however, they are complex and economically unfavorable due to the maintenance and sterilization. Alternatively, anaerobic fermentation with mixed microbial consortium has attracted increasing interest due to its sustainable resource recycling and cost-effectiveness (Liang et al. 2015, Rafieenia et al. 2018).

Food waste (FW), posing public and environmental health concerns, is generated in the amount of more than one billion tons annually (Gunasekera 2015, Ko et al. 2018). A few studies showed synergistic effects on enhancements of hydrolysis and acidification during co-fermentation of FW and waste activated sludge (WAS) from municipal wastewater treatment plants (Fitamo et al. 2016, Zhang et al. 2017). However, LA is a metabolizing intermediate and easily converted to volatile fatty acids (VFA) by mixed microbial consortium. Among two enantiomers of LA, i.e. D- and L-LA, the latter one is preferentially converted to other metabolites, while decreasing L-LA yield and OA (Li et al. 2016, Zhang et al. 2020). Although supplementation with iron and

copper ion partially inhibited VFA production and stabilized LA accumulation (Li et al. 2017, Ye et al. 2018), these exogenous metal ions inevitably increased maintenance cost. It is thus appealing to develop a more reliable and chemically-independent approach to maintain stable L-LA production with the recovery of highly valuable fermentation products.

It is worth noting that the content of salt in FW is around 2%-5%. The accumulated salt exerts osmotic pressure that affects fermentation process (Huang et al. 2019a, Li et al. 2019). For example, methane production decreased by more than 90% at the salinity above 30 mS cm^{-1}, resulting in VFA accumulation (De Vrieze et al. 2016). The reported inhibition thresholds for VFA generation ranged from 16 to even 70 g NaCl/L under different fermentation conditions (He et al. 2019, Zhao et al. 2016). Therefore, stabilization of lactate accumulation remains unclear at high salinity. Normally, transient lactate accumulation was widely observed in the early stages of fermentation for VFA production (Li et al. 2016, Tamis et al. 2015). This effect was attributed to the reduction of pyruvate by nicotinamide adenine dinucleotide (NADH) through lactate dehydrogenase (*ldh*) (Zhang et al. 2020). In contrast, a simultaneous increase in both lactate and VFA (mainly propionate) was observed in hydrogen fermentation at 53.4 g NaCl/L (Kim et al. 2009). That finding suggests that salt could be an overlooked factor impacting the commonly recognized relationship between LA consumption and VFA generation. Especially, the effect of salinity on OA-L remains largely unknown. The activity of specific D-lactate dehydrogenase (*ldhD*), which is responsible for D-LA production, is more vulnerable to chemical inhibition than L-

lactate producing enzyme (Li et al. 2017, Zhang et al. 2020). It is thus reasonable to hypothesize that a high salinity content of FW may be beneficial for optically active L-LA production. Nevertheless, there is still an unclear role of salt in regulating high optical active L-LA production during co-fermentation of FW and WAS.

Recently, it has been reported that microorganisms from WAS eventually outcompeted LAB during long-term microbiome acclimatization from FW and sludge (Xu et al. 2019, Zhang et al. 2020). High salinity inevitably inhibited specific microbial activities due to the acute toxicity and high osmotic pressure, thus leading to a shift in microbial community along with the fermentation time (Shi et al. 2015). Specifically, little is known about how salinity impacts the abundance of LAB and key functional genes related to LA production, such as L-lactate dehydrogenases (*ldhL*) and *ldhD*. Thus, unveiling the underlying mechanism of salt on mixed culture fermentation is important for optimization of the recovery of the valuable platform molecule from FW.

Therefore, this study proposes a reliable approach to improve high value-added platform molecule (L-LA) production and shape the functional LAB during co-fermentation of FW and WAS. First, the LA production and OA-L were compared for the co-substrates with different salinity. The interactive effect of salt concentration and fermentation time was analyzed using the response surface methodology (RSM). Then, the correlation between LA generation and competing VFA production were evaluated. The substrate utilization efficiency was also analyzed including three steps: solubilization, hydrolysis, and glycolysis. Furthermore, a shift in the microbial community under different salinity conditions and fermentation times was also

investigated. Finally, the relationship between salinity, key LAB, and functional genes was evaluated by network analysis and redundancy analysis (RDA).

2. Materials and methods

2.1. Origin and characteristics of the mixed substrate (FW and WAS)

FW, mainly composed of meat, rice, vegetables, and tofu, was withdrawn from a canteen in Donghua University (Shanghai, China). The FW was washed three times with tap water (centrifuging and removing the supernatant) to eliminate the inherent salinity. Then, the FW was milled using a blender, diluted to slurry state with tap water, and stored at 4°C prior to the use. WAS was withdrawn from a municipal wastewater treatment plant (Shanghai, China) and then settled for 24 h at 4°C to obtain the concentrated sludge. The FW and WAS were mixed to obtain a volatile suspended solid (VSS) ratio VSS_{FW}/VSS_{WAS} = 6:1, similar to our previous study (Li et al. 2015). Then, a given volume of tap water was added to the mixture to adjust total chemical oxygen demand (TCOD) of the co-fermentation substrate at 40 g COD/L. The total dissolved solids (TDS) concentration of tap water was around 250 mg/L, which was negligible compared to the lowest salt dosage to Reactor-10 (10 g NaCl /L). The characteristics of the FW, WAS and mixed substrate is presented in Table 1.

2.2. Co-fermentation of substrates with different salinity

Six reactors (sealed to ensure anaerobic condition) in triplicate, containing 0.8 L

(total volume 1L) co-fermentation substrate, were amended with NaCl at the following dosages: 0 (blank reactor), 10 g/L (R-10), 20 g/L (R-20), 30 g/L (R-30), 40 g/L (R-40), and 50 g/L (R-50). All the reactors were stirred mechanically (120 rpm) and maintained at 50 ± 1°C in the water bath similar to our previous study (Li et al. 2018). The pH was controlled at 7.0 ± 0.1 by the addition of 5 M NaOH solution or 5 M HCl solution every 8 h. Samples were withdrawn from the reactors every 24 hours, centrifuged at 8000 rpm for 10 min, and then filtered by membrane filters (pore size of 0.45 μm) for subsequent chemical analysis. The concentrations of LA isomers (L-LA and D-LA), VFA, NH_4^+-N, protein, and carbohydrates were assayed. The increase in soluble chemical oxygen demand (SCOD), reduction of VSS, and the relative activities of α-glucosidase and protease were determined to evaluate the efficiency of solubilization and hydrolysis during co-fermentation. The carbon balance was calculated based on the contribution of SCOD of carbonaceous substances on day 3 and day 7. The correlation of incremental LA and VFA production was evaluated for phase 1 (day 0-3) and phase 2 (day 3-7).

2.3. Optimization of L-lactate fermentation by RSM

The interaction effects of salt concentration and fermentation time on the maximum concentration of LA were evaluated by Design Expert Software (version 10) with a central composite design (CCD). Table 2 shows the coded levels of the independent factors (salt concentration and fermentation time). The R-square was used to compare the predictive ability of models (described in Part 3.1) by the following

formula:

$$\text{R-square} = 1 - SS_{Residual}/(SS_{Residual} + SS_{Model}) \quad (1)$$

where $SS_{Residual}$ and SS_{Model} is the sum of squares of the residual and model, respectively.

2.4. Utilizing pyruvate and NADH as substrate catalyzed by cell extract for ex-situ lactate production

The reduction of pyruvate to lactate was depended on the electron donor of NADH (based on the gene *ldh*) and ferrocytochrome c (based on the gene *ldh* (cytochrome)). The protocols for the determination of *ldhL* and *ldhD* were adapted from (Diezgonzalez et al. 1995) to evaluate the effect of *ldh* on LA production. 30 ml aliquots of fermentation mixture samples were collected on day 3 from all the reactors. The samples were washed by centrifugation (10000 G, 4 ºC, 10 min), followed by resuspension with 50 mM Tris-HCl buffer (total volume 20 ml). Cells were obtained after repeating the washing process 3 times and then disrupted by sonication (ice-bath) for 30 min (total volume 15 ml). The cell extracts were placed in sealed centrifuge tubes (50 ml), and the cell debris was removed by centrifugation at 10000 G for 30 min. The cell-free extract was stored in sealed vials at T = 4 ºC. The lactate fermentation pathway was described by *Eq (2)* as in the previous study (Li et al. 2015). 0.5 ml pyruvate (80 mM), 0.25 ml NADH (8 mM), and 0.5 ml cell-free extract were mixed for LA production to reflect the relative activity of *ldh*.

$$pyruvic\ acid + NADH \overset{ldhL/ldhD}{\Longleftrightarrow} L-LA/D-LA + NAD^{+} \quad (2)$$

2.5. Analysis of microbial community structures and functional genes

Illumina Miseq pyrosequencing method was used to investigate microbial community structure. Samples from the blank reactor, R-10 (maximum LA production), and R-30 (maximum pure L-LA production) were collected respectively on day 3 and day 7 for 16S rRNA sequence (detailed in Part 3.1). Methanogens was not investigated in this study due to the focus on aqueous fermentation products rather than biogas. The extracted DNA from each of the triplicate samples was pooled together to reduce the potential variation and then amplified by polymerase chain reaction using primers 806R (5'-GGACTACHVGGGTWTCTAAT-3') and 338F (5'-ACTCCTACGGGAGGCAGCA-3') in the V3-V4 region. The functional profiles of microbial communities were based on the Kyoto Encyclopedia of Genes and Genomes (KEGG) Pathway Database. All the raw sequences were deposited in the NCBI Short Read Archive database under the accession numbers SRR9590820, SRR9590821 and SRR9590822.

2.6. Analytical methods

The LA isomers (L-LA and D-LA) were determined by a high-performance liquid chromatograph (HPLC) (Thermol Ultimate 3000). The equipped column was Astec CLC-D (5 mm, 15 cm × 4.6 mm). The determination of wavelength was set at 254 UV. 5 mM $CuSO_4$ solution was used as the mobile phase of the HPLC with a flow rate at 1.0 mL/min. Gas chromatography (GC) (Agilent GC 7820), equipped with a flame ionization detector and a DB-WAX column (30 m×1.0 mm×0.53 mm), was used to

determine the VFA concentrations. The SCOD, carbohydrate, protein, total suspended solids (TSS), VSS, NH_4^+-N, and hydrolase (α-glucosidase and protease) were measured as described previously (Li et al., 2015; Zhang et al., 2017).

2.7. Calculation

The OA-L (%) was defined as follows:

$$OA = ([L] - [D]) / ([L] + [D]) \times 100\% \quad (3)$$

where [L] and [D] represented the concentrations of L-LA and D-LA, respectively.

2.8. Statistical analysis

R (version 3.6.3) software environment for statistical computing and graphics was used to assess the correlation between microbial communities and environmental factors by RDA. The network correlation graphs were created by Cytoscape 3.6.0 based on strong correlations (Spearman's r2 > 0.8 and $p< 0.05$). All the chemical results were expressed as the mean ± standard deviation (in triplicate). The analysis of variance (ANOVA) was used to evaluated the significance of results, where $p<0.05$ was considered to be statistically significant.

3. Results and Discussion

3.1. Increased L-LA production and optical activity in high salinity and fermentation parameter optimization by RSM

The LA concentration increased to 15.1 ± 1.7 g/L in the blank reactor at day 3, and then gradually depleted (Fig. 1A). This behavior was similar to our previous studies conducted under thermophilic conditions (Zhang et al. 2017). With the increase of salt concentration from 10 g/L (R-10) to 40 g/L (R-40), the maximum concentrations of LA were increased to 29.5 ± 1.7 (obtained on day 2), 22.9 ± 1.5 (day 3), 25.5 ± 1.6 (day 7) and 21.7 ± 1.1 (day 7). However, the LA production was inhibited significantly at R-50 with the peak value being only 7.9 ± 2.0 g/L on day 4. Moreover, the highest productivity (14.7 g/(L·d)) was also observed in R-10, revealing a 1.9-fold increase compared to the blank reactor. LA production increased significantly in R-20 and R-30 compared to the blank reactor on day 3 and then maintained at a stable level. In R-40, the LA production also increased while its productivity decreased during the whole fermentation period. However, further increasing salinity to 50 g NaCl/L inhibited the LA production. In the literature, a promoted LA production was also observed even under the condition of 70 g NaCl/L followed by a quick depletion subsequently under mesophilic conditions (He et al. 2019).

The maximum concentrations of LA isomers were 12.8 ± 1.2 g/L (L-LA on day 2) and 6.5 ± 1.0 g/L (D-LA on day 3) in the blank reactor (Fig. 1B and 1C). The increase in D-LA (12.5 ± 1.2 g COD/L) in R-10 explained the decline of OA-L (Fig. 1D).

However, with the increase in salinity from 20 g NaCl/L to 50 g NaCl/L, the production of D-LA was inhibited (Fig. 1C), resulting in high OA of L-LA in these reactors (R-20 to R-50 in Fig. 1D). This may implicitly be related to the vulnerability of D-lactate producing enzymes to chemical inhibitors, such as alkaline, ammonia, and copper ion (Li et al. 2015, Ye et al. 2018, Zhang et al. 2020). It was discovered for the first time that OA-L could be enhanced under hypersaline conditions.

The interaction effects of salt dosage and fermentation time on L-LA and D-LA production was verified using RSM. With the quadratic models, the predicted maximal L-LA production was 24.7 g/L under 31.7 g NaCl/L at 4.7 d. In addition, under specific conditions, i.e. NaCl concentration of 11.7 g/L and fermentation time of 5 d, the lowest OA-L may be obtained due to the enhanced D-LA generation. Thus, it is possible to obtain optical pure L-LA from FW with high salinity rather than exogenous chemical addition, providing a cost-effective and reliable approach for efficient L-LA production.

3.2. VFA production and correlation analysis between increased LA and VFA production with salinity

The VFA production increased in R-10 (12.0 ± 1.5 g COD/L) and R-20 (12.4 ± 1.1g COD/L) compared to the blank reactor (7.4 ± 1.4 g COD/L), but decreased (7.2 to 7.5 g COD/L) in R-30, R-40 and R-50 (Fig. 2). In addition to the production rate, the fermentation pathway and composition of VFA also changed significantly under different salinity levels. Valerate and butyrate dominated in the blank reactor, R-10, and R-20 (Fig. 2A-2C), whereas the dominant VFA shifted to acetate in R-30, R-40, and R-

50 (Fig. 2D-2F). In the literature (20 ºC at pH 7), the VFA content and proportions were as follows: propionate > acetate > butyrate > valerate under saline condition (Zhao et al. 2016). However, VFA with dominated acetate was reported under saline condition (30 ºC at pH 6) (He et al. 2019). In our previous study, the thermophilic temperature (T = 50 ºC) was favorable for both acetate and butyrate production, while propionate production was inhibited (Zhang et al. 2017). That finding was different from the blank reactor in this study, possibly due to the washed FW from the blank reactor. In summary, the interactive effects of fermentation temperature and salt concentration on VFA production and composition requires further investigation.

The carbon components in the fermentation liquid mainly consisted of LA and VFA according to the carbon balance analysis. It is commonly recognized that LA is easily converted to VFA during fermentation (Tamis et al. 2015, Zhang et al. 2020). However, positive correlations were observed between increased LA and VFA (mainly butyrate and valerate) production from day 0 to 3 (Fig. 3A), indicating that LA and VFA production competed on the substrates during the first 3 days of fermentation. Moreover, the appropriate salt concentrations (10 to 30 g NaCl/L) enhanced the production of both LA and VFA. Further increasing salt concentration impaired the production of both LA and VFA in R-40 and R-50. Negative correlations were observed between LA and VFA production in the blank reactor, R-10 and R-20 from day 3 to 7 (Fig. 3B), which indicates that LA was utilized and converted to VFA (mainly butyrate and valerate) in these reactors. Nevertheless, the positive correlation between LA and VFA (mainly acetate) production remained the same in the reactors with the higher salt

concentrations (R-30, R-40, and R-50) from day 3 to 7. This could be caused by higher amounts of carbohydrates remaining in these reactors compared to the blank reactor, R-10, and R-20. The higher concentrations of carbohydrates in the reactors with high salt amendment might weaken the consumption of LA for VFA production. It is thus imperative to understand the effect of salt on substrate utilization.

3.3. Substrate utilization altered by salinity

Fermentation normally consists of solubilization, hydrolysis, glycolysis and acidification (Zhang et al. 2020), followed by subsequent methanogenesis. The rate of substrate utilization (including solubilization, hydrolysis, and glycolysis) is crucial for LA production. Substrates in the liquid phase could be assimilated by microorganisms after being solubilized from the solid phase. The improved VSS reduction (23.4 ± 5.4 %) and increased SCOD production (7 ± 3 %) were observed in the reactors amended with salt (Fig. 4A and 4B), indicating the increase in solubilization under salinity conditions. The presence of salt might accelerate the release of soluble fermentative substances from FW and disruption of both extracellular polymers substances (EPS) and cell envelopes from WAS (Zhao et al. 2016).

Generally, hydrolysis is regarded as the rate-limiting step in anaerobic fermentation. Soluble polysaccharides are hydrolyzed to monosaccharides by α-glucosidase, while soluble proteins are hydrolyzed to amino acids by protease (Kavitha et al. 2016, Liu and Chen 2018, Luo et al. 2020). The relative activity of α-glucosidase

and protease increased from the blank reactor to R-10 but then gradually decreased to R-40 and R-50 (Fig. 4C and 4D), indicating that the hydrolysis process was enhanced most in R-10. This coincided with the maximal productivity of LA in R-10.

It should be noted that the major component of the co-substrates were carbohydrates. Their initial concentration in the reactors exceeded 30 g COD/L. The carbohydrates consumption (glycolysis) at the lower salt concentrations (R-10 and R-20) was similar to the blank reactor. However, the activity of glycolysis (related to the subsequent LA production) decreased in R-30 and R-40 (by approximately 20%), and even more in R-50 (by approximately 50%) (Fig. 4E).

Protein is crucial for microbial growth and propagation (Surmann et al. 2020). Although the concentration of protein maintained at a lower level (<0.4 g COD/L) during fermentation. The average protein concentration increased gradually with the increasing salt dosages. This might implicitly be caused by acute cell lysis and protein release to the liquid phase induced in the hypersaline environment. Ammonium, a biostimulator for a biorefinery of organic wastes (Zhang et al. 2020, Zhao et al. 2018), decreased in the blank reactor, R-10, R-20, and R-30 from day 0 to day 3. This might be due to the ammonium utilization (assimilation) by microorganisms in these reactors (Fig. 4F). In contrast, the concentration of ammonium increased under hypersaline conditions (R-40 and R-50) from day 0 to day 3. This indicates that ammonium utilization might be impaired under hypersaline condition during the initial fermentation phase.

From the carbon mass balance analysis, it appears that ethanol was only observed

at R-40 and R-50 on day 7, indicating that lactate fermentation pathway shifted from Embden-Meyerhof pathway (1 mol glucose for 2 mol LA) to phosphoketolase or heterolactic pathway (1 mol glucose for 1 mol LA and 1 mol ethanol) (Burge et al. 2015). In addition, the concentration of unknown organic substance increased under high salinity, which might be attributed to the organic molecules, called compatible solutes, synthesized by microbial cells for adapting to high osmotic pressure (Sudmalis et al. 2018).

3.4. Effects of salt dosage on the microbial community

The microbial community structure highly determined the performance of LA production during the co-fermentation of FW and WAS. The rarefaction curve indicated that the sequencing results were sufficient to reflect the diversity in the current samples. On day 3, the microbial richness was higher in R-10 compared to R-30 according to the variation of alpha-diversity indices (Chao1 and Ace) (Table 3). The salt concentration at 10 g NaCl/L was favorable for the growth and propagation of microorganisms from WAS, while the high salt concentration (30 g NaCl/L) caused the death of those microorganisms due to the increased osmotic pressure (Lefebvre and Moletta 2006). Moreover, the microbial richness increased by 53.1% (Chao1) and 54.6% (Ace) in the blank reactor on day 7 compared to day 3. However, in the other reactors, the increased microbial richness was lower on day 7 compared to day 3, i.e. 9.2% (Chao1) and 2.5% (Ace) in R-10, and 34.7% (Chao1) and 44.9% (Ace) in R-30. The reactors operated

with salinity, especially R-10, exhibited less richness discrepancy between day 3 and day 7. In addition, those reactors also exhibited a decreased diversity compared to the blank reactor in terms of Simpson (with non-significance) and Shannon indices (Table 3). This was due to the selective pressure of salinity in the initial fermentation stage to suppress microorganisms (without salinity resistance).

The distribution of community at the phylum level was mainly affiliated to *Firmicutes, Proteobacteria, Actinobacteria*, and *Saccharibacteria*. They are commonly present in WAS and responsible for the complex organic substance degradation and (She et al. 2020, Zheng et al. 2013). The relative abundance of *Firmicutes* (the dominant phylum) accounted for 97.0% (3 d) and 98.7% (7 d) in the blank reactor, 75.0% (3 d) and 94.5% (7 d) in R-10, 67.4% (3 d) and 72.9% (7 d) in R-30, respectively. The salt addition (10 and 30 g NaCl/L) facilitated the proliferation of *Proteobacteria, Actinobacteria*, and *Saccharibacteria,* while resulted in decreasing the relative abundance of *Firmicutes*. At the genus level, the key LAB, including *Bacillus, Enterococcus, Lactobacillus* (Li et al. 2018, Zhang et al. 2020), and VFA producers, including *Tepidimicrobium, Clostridium, Tepidibacter, Proteiniborus* (Choi et al. 2012, Huang et al. 2019b, Urios et al. 2004, Wang et al. 2019), were observed as shown Fig. 5.

The LA concentration increased only by 1.09 g/L from day 2 to day 3 in the blank reactor (Fig. 1A), indicating that the peak value for LA production occurred probably between day 2 and day 3. It is thus to prove that the LA has been consumed on day 3 which was in a good agreement with the abundance of the dominating *Clostridium*

(85%) in the blank reactor on day 3. Furthermore, the relative abundance of LAB increased, which facilitated and stabilized LA production (Fig. 1A). The increases of LAB were ranged from 8% (the blank reactor) to 71% (R-10) on day 3, and from 1% (the blank reactor) to 7% (R-10) on day 7. *Lactobacillus,* enable to produce both L-LA and D-LA (Li et al. 2018, Zhang et al. 2017), dominated on day 3 accounting for 44%. Their high relative abundance corresponded to the low OA of L-LA in R-10 (Fig. 1D). Particularly, the relative abundance of LAB increased from 8% (the blank reactor) to 62% (R-30) on day 3, and from 1% (the blank reactor) to 62% (R-30) on day 7 in R-30. *Bacillus and Enterococcus,* which were reported to specifically produce optically pure L-LA (Zhang et al. 2020), dominated in R-30 accounting for 60%. The high relative abundance of LAB (for pure L-LA production) in R-30 may be the main explanation for the optical pure L-LA (Fig. 1).

3.5. Correlation among microbial communities, KEGG predicted functional genes and salinity

Correlation between the key LAB (*Bacillus* and *Enterococcus*), VFA producer (*Clostridium*), and fermentation parameters (salinity, LA production, and fermentation time) were evaluated by RDA (Fig. 6A). The first and the second ordination axes could explain 58.44% and 18.16% of the microbial community variations. There were positive correlations between the key LAB (*Bacillus* and *Enterococcus*), salinity, and LA production, indicating that salinity was favorable to the proliferation of key LAB

(*Bacillus* and *Enterococcus*) to facilitate LA production. *Clostridium,* the potential competitor of the LAB for substrates, was negatively correlated with the key LAB (*Bacillus* and *Enterococcus*), salinity, and LA production. It was evident that the out-selection of *Clostridium* occurred due to salinity inhibition (Fig. 5). Furthermore, the network analysis suggested that variation of KEGG predicted functional genes and salinity were strongly associated with changes in the microbial community structure (Fig. 6B). There was explicitly a positive correlation between salinity and the key LAB (*Bacillus* and *Enterococcus*), capable of thriving under hypersaline conditions (Kang et al. 2020, Lee et al. 2016). In addition, salinity and *Bacillus* were positively correlated with transport and catabolism, indicating that the transport and catabolism were enhanced by salt addition, possibly due to the increasing relative abundance of *Bacillus* (Fig. 5).

A positive correlation among *Lactobacillus*, *ldhL*, and *ldhD* (Fig. 6B) indicates that the expression of *ldhL* and *ldhD* were mainly attributed to *Lactobacillus*, which dominated in R-10. Additionally, the relative abundance of *ldhL* and *ldhD* increased in R-10 compared to the blank reactor and R-30 (left in Fig. 6C), which was consistent with the higher LA production (Fig. 1A) and relative higher abundance of *Lactobacillus* in R-10 compared to the blank reactor and R-30. However, the decreased abundance of *ldhL* was not consistent with the increased L-LA production in R-30 (Fig. 1B). Interestingly, the highest relative abundance of *ldhL* (cytochrome), which utilized the ferrocytochrome c as the electron donor (Smutok et al. 2013) (*Eq. 4*), was observed in R-30 compared to the blank reactor and R-10 (right in Fig. 6C). Moreover, *ldhL*

(cytochrome) was positively correlated with *Enterococcus* and salinity (Fig. 6B). This was consistent with the increased relative abundance of *Enterococcus* in R-30 compared to the blank reactor and R-10 (Fig. 5). Thus, the fermentation pathway for L-LA might implicitly be dependent on the role of the function gene *ldhL* (cytochrome) under hypersaline conditions. The traditional LA functional genes of *ldhL or ldhD* determine the reduction of pyruvate by using electron donor NADH (*Eq. 2*). Thus, an ex-site test was carried out to mimic the reduction of pyruvate using NADH catalyzed by the cell extract from the blank reactor, R-10 and R-30 (left in Fig. 6D). The variation of LA isomers yield was similar to the tendency of *ldhL* and *ldhD* (left in Fig. 6C). This verified that the relative activities of *ldhL* and *ldhD* (NADH dependent) were enhanced in R-10, but decreased in R-30. However, the co-fermentation from FW and WAS showed the tendency to increase the L-LA yield and complete inhibition of the D-LA yield (right in Fig. 6D), similar to the patterns of *ldhL* (cytochrome) (right in Fig. 6C). This study unveiled that another overlooked LA function gene *ldhL* (cytochrome) could also play an important role in L-LA production:

$$pyruvic\ acid + 2\ ferrocytochrome\ c + 2\ H(+) \xleftrightarrow{ldhL(cyt)/ldhD(cyt)} L-LA/D-LA + 2\ ferricytochrome\ c \quad (4)$$

4. Conclusion

This study proposed a sustainable approach for optical pure L-lactate production by regulating salinity. This was due to the increased solubilization and hydrolase activities under saline conditions. In addition, high salinity changed the common

conversion of LA to VFA, thus leading to the accumulation of LA. Moreover, the key LAB thrived under saline conditions and increased their relative abundance. The traditional functional genes for L-lactate production were highly dependent on another overlooked functional gene *ldh* (cytochrome) at 30 g NaCl/L, providing a novel insight into the recovery of value-added platform molecules from organic wastes.

Acknowledgments

The author acknowledges the financial support from the National Natural Science Foundation of China (NSFC) (Grant NO. 51878137); National Key R&D Program of China (No. 2019YFD1100502); Shanghai Rising-Star Program (20QA1400400). Fundamental Research Funds for the Central Universities and the Donghua University Distinguished Young Professor Program.

Reference

[1] Burge, G., Saulou-Berion, C., Moussa, M., Allais, F., Athes, V. and Spinnler, H.E. (2015) Relationships between the use of Embden Meyerhof pathway (EMP) or Phosphoketolase pathway (PKP) and lactate production capabilities of diverse Lactobacillus reuteri strains. J. Microbiol. 53(10), 702-710.

[2] Choi, O., Um, Y. and Sang, B.-I. (2012) Butyrate production enhancement by Clostridium tyrobutyricum using electron mediators and a cathodic electron donor. Biotechnol. Bioeng. 109(10),

2494-2502.

[3] De Vrieze, J., Coma, M., Debeuckelaere, M., Van der Meeren, P. and Rabaey, K. (2016) High salinity in molasses wastewaters shifts anaerobic digestion to carboxylate production. Water Res. 98, 293-301.

[4] Diezgonzalez, F., Russell, J.B. and Hunter, J.B. (1995) The role of an NAD-independent lactate-dehydrogenase and acetate in the utilization of lactate by Clostridium-acetobutylicum strain P262. Arch. Microbiol. 164(1), 36-42.

[5] Fitamo, T., Boldrin, A., Boe, K., Angelidaki, I. and Scheutz, C. (2016) Co-digestion of food and garden waste with mixed sludge from wastewater treatment in continuously stirred tank reactors. Bioresource. Technol. 206, 245-254.

[6] Gunasekera, D. (2015) Cut food waste to help feed world. Nature 524(7566), 415-415.

[7] He, X., Yin, J., Liu, J., Chen, T. and Shen, D. (2019) Characteristics of acidogenic fermentation for volatile fatty acid production from food waste at high concentrations of NaCl. Bioresource. Technol. 271, 244-250.

[8] Huang, L., Fu, X.-Z., Cui, S., Liu, H.-Q., Yu, H.-Q. and Li, W.-W. (2019a) Intracellular polymers production in anaerobic sludge under salt shock and batch fermentation conditions: Experimental and modelling study. Biochem. Eng. J. 142, 68-73.

[9] Huang, Y., Wang, Y., Liu, S., Huang, W., He, L. and Zhou, J. (2019b) Enhanced hydrolysis-acidification of high-solids and low-organic-content sludge by biological thermal-alkaline synergism. Bioresource. Technol. 294.

[10] Kang, H., Kang, J., Cha, I., Kim, H., Joung, Y., Jang, T.Y. and Joh, K. (2020) Bacillus salinus sp. nov., isolated from commercial solar salt. INT. J. SYST. EVOL. MICR.

[11] Kavitha, S., Banu, J.R., Kumar, J.V. and Rajkumar, M. (2016) Improving the biogas production performance of municipal waste activated sludge via disperser induced microwave disintegration. Bioresource. Technol. 217, 21-27.

[12] Kim, D.-H., Kim, S.-H. and Shin, H.-S. (2009) Sodium inhibition of fermentatlive hydrogen production. International Journal of Hydrogen Energy 34(8), 3295-3304.

[13] Ko, J.H., Wang, N., Yuan, T., Lu, F., He, P. and Xu, Q. (2018) Effect of nickel-containing activated carbon on food waste anaerobic digestion. Bioresource. Technol. 266, 516-523.

[14] Lee, H., Gwak, E., Lee, S., Kim, S., Lee, J., Ha, J., Oh, M.-h., Park, B.-y., Yang, M., Choi, K.-h. and Yoon, Y. (2016) Model to Predict Growth/No Growth Interfaces of Enterococcus as A Function of NACl and NANO(2). J. Food. Safety. 36(4), 537-547.

[15] Lefebvre, O. and Moletta, R. (2006) Treatment of organic pollution in industrial saline wastewater: A literature review. Water Res. 40(20), 3671-3682.

[16] Li, J., Zhang, W., Li, X., Ye, T., Gan, Y., Zhang, A., Chen, H., Xue, G. and Liu, Y. (2018) Production of lactic acid from thermal pretreated food waste through the fermentation of waste activated sludge: Effects of substrate and thermal pretreatment temperature. Bioresource. Technol. 247, 890-896.

[17] Li, X., Chen, Y., Zhao, S., Chen, H., Zheng, X., Luo, J. and Liu, Y. (2015) Efficient production of optically pure L-lactic acid from food waste at ambient temperature by regulating key enzyme activity. Water Res. 70, 148-157.

[18] Li, X., Huang, J., Liu, Y., Huang, T., Maurer, C. and Kranert, M. (2019) Effects of Salt on Anaerobic Digestion of Food Waste with Different Component Characteristics and Fermentation Concentrations. Energies 12(18).

[19] Li, X., Zhang, W., Ma, L., Lai, S., Zhao, S., Chen, Y. and Liu, Y. (2016) Improved production of

propionic acid driven by hydrolyzed liquid containing high concentration of L-lactic acid from co-fermentation of food waste and sludge. Bioresource. Technol. 220, 523-529.

[20] Li, X., Zhang, W., Xue, S., Lai, S., Li, J., Chen, H., Liu, Z. and Xue, G. (2017) Enrichment of D-lactic acid from organic wastes catalyzed by zero-valent iron: an approach for sustainable lactate isomerization. Green Chem. 19(4), 928-936.

[21] Liang, S., McDonald, A.G. and Coats, E.R. (2015) Lactic acid production from potato peel waste by anaerobic sequencing batch fermentation using undefined mixed culture. Waste Manage. 45, 51-56.

[22] Liu, H. and Chen, Y. (2018) Enhanced Methane Production from Food Waste Using Cysteine To Increase Biotransformation of L-Monosaccharide, Volatile Fatty Acids, and Biohydrogen. Environ. Sci. Technol. 52(6), 3777-3785.

[23] Lunt, J. (1998) Large-scale production, properties and commercial applications of polylactic acid polymers. Polym. Degrad. Stabil. 59(1-3), 145-152.

[24] Luo, J., Zhang, Q., Zha, J., Wu, Y., Wu, L., Li, H., Tang, M., Sun, Y., Guo, W., Feng, Q., Cao, J. and Wang, D. (2020) Potential influences of exogenous pollutants occurred in waste activated sludge on anaerobic digestion: A review. Journal of Hazardous Materials 383.

[25] Lv, S., Zhang, Y. and Tan, H. (2019) Thermal and thermo-oxidative degradation kinetics and characteristics of poly (lactic acid) and its composites. Waste Manage. 87, 335-344.

[26] Meng, Y., Xue, Y., Yu, B., Gao, C. and Ma, Y. (2012) Efficient production of L-lactic acid with high optical purity by alkaliphilic Bacillus sp WL-S20. Bioresource. Technol. 116, 334-339.

[27] Pejin, J., Radosavljevic, M., Pribic, M., Kocic-Tanackov, S., Mladenovic, D., Djukic-Vukovic, A. and Mojovic, L. (2018) Possibility of L-(+)-lactic acid fermentation using malting, brewing, and oil

production by-products. Waste Manage. 79, 153-163.

[28] Rafieenia, R., Pivato, A., Lavagnolo, M.C. and Cossu, R. (2018) Pre-treating anaerobic mixed microflora with waste frying oil: A novel method to inhibit hydrogen consumption. Waste Manage. 71, 129-136.

[29] She, Y., Hong, J., Zhang, Q., Chen, B.-Y., Wei, W. and Xin, X. (2020) Revealing microbial mechanism associated with volatile fatty acids production in anaerobic acidogenesis of waste activated sludge enhanced by freezing/thawing pretreatment. Bioresource. Technol. 302.

[30] Shi, X., Ng, K.K., Li, X.-R. and Ng, H.Y. (2015) Investigation of Intertidal Wetland Sediment as a Novel Inoculation Source for Anaerobic Saline Wastewater Treatment. Environ. Sci. Technol. 49(10), 6231-6239.

[31] Smutok, O., Karkovska, M., Smutok, H. and Gonchar, M. (2013) Flavocytochrome b_2-based enzymatic method of L-lactate assay in food products. Sci. World. J. 2013, 461284-461284.

[32] Sudmalis, D., Millah, S.K., Gagliano, M.C., Butre, C.I., Plugge, C.M., Rijnaarts, H.H.M., Zeeman, G. and Temmink, H. (2018) The potential of osmolytes and their precursors to alleviate osmotic stress of anaerobic granular sludge. Water Res. 147, 142-151.

[33] Surmann, K., Stopp, M., Woerner, S., Dhople, V.M., Voelker, U., Unden, G. and Hammer, E. (2020) Fumarate dependent protein composition under aerobic and anaerobic growth conditions in Escherichia coli. Journal of Proteomics 212.

[34] Tamis, J., Joosse, B.M., van Loosdrecht, M.C.M. and Kleerebezem, R. (2015) High-rate volatile fatty acid (VFA) production by a granular sludge process at low pH. Biotechnol. Bioeng. 112(11), 2248-2255.

[35] Urios, L., Cueff, V., Pignet, P. and Barbier, G. (2004) Tepidibacter formicigenes sp nov., a novel

spore-forming bacterium isolated from a Mid-Atlantic Ridge hydrothermal vent. INT. J. SYST. EVOL. MICR. 54, 439-443.

[36] Wang, X., Li, Y., Zhang, Y., Pan, Y.-R., Li, L., Liu, J. and Butler, D. (2019) Stepwise pH control to promote synergy of chemical and biological processes for augmenting short-chain fatty acid production from anaerobic sludge fermentation. Water Res. 155, 193-203.

[37] Xu, X., Zhang, W., Gu, X., Guo, Z., Song, J., Zhu, D., Liu, Y., Liu, Y., Xue, G., Li, X. and Makinia, J. (2019) Stabilizing lactate production through repeated batch fermentation of food waste and waste activated sludge. Bioresource. Technol. 300, 122709-122709.

[38] Ye, L., Zhou, X., Bin Hudari, M.S., Li, Z. and Wu, J.C. (2013) Highly efficient production of L-lactic acid from xylose by newly isolated Bacillus coagulans C106. Bioresource. Technol. 132, 38-44.

[39] Ye, T., Li, X., Zhang, T., Su, Y., Zhang, W., Li, J., Gan, Y., Zhang, A., Liu, Y. and Xue, G. (2018) Copper (II) addition to accelerate lactic acid production from co-fermentation of food waste and waste activated sludge: Understanding of the corresponding metabolisms, microbial community and predictive functional profiling. Waste Manage. 76, 414-422.

[40] Zhang, W., Li, X., Zhang, T., Li, J., Lai, S., Chen, H., Gao, P. and Xue, G. (2017) High-rate lactic acid production from food waste and waste activated sludge via interactive control of pH adjustment and fermentation temperature. Chem. Eng. J. 328, 197-206.

[41] Zhang, W., Xu, X., Yu, P., Zuo, P., He, Y., Chen, H., Liu, Y., Xue, G., Li, X. and Alvarez, P.J.J. (2020) Ammonium Enhances Food Waste Fermentation to High-Value Optically Active L-Lactic acid. Acs Sustain. Chem. Eng. 8(1), 669-677.

[42] Zhao, J., Liu, Y., Wang, Y., Lian, Y., Wang, Q., Yang, Q., Wang, D., Xie, G.-J., Zeng, G., Sun, Y., Li,

X. and Ni, B.-J. (2018) Clarifying the Role of Free Ammonia in the Production of Short-Chain Fatty Acids from Waste Activated Sludge Anaerobic Fermentation. Acs Sustain. Chem. Eng. 6(11), 14104-14113.

[43] Zhao, J., Zhang, C., Wang, D., Li, X., An, H., Xie, T., Chen, F., Xu, Q., Sun, Y., Zeng, G. and Yang, Q. (2016) Revealing the Underlying Mechanisms of How Sodium Chloride Affects Short-Chain Fatty Acid Production from the Cofermentation of Waste Activated Sludge and Food Waste. Acs Sustain. Chem. Eng. 4(9), 4675-4684.

[44] Zheng, X., Su, Y., Li, X., Xiao, N., Wang, D. and Chen, Y. (2013) Pyrosequencing Reveals the Key Microorganisms Involved in Sludge Alkaline Fermentation for Efficient Short-Chain Fatty Acids Production. Environ. Sci. Technol. 47(9), 4262-4268.

Table 1

Characteristics of FW, WAS, and the mixed substrate for co-fermentation.

	FW	WAS	Mixed substrate [a]
pH	6.8 ± 0.4	6.6 ± 0.2	7.0 ± 0.2
TSS (g/L)	125.6 ± 5.4	15.6 ± 2.1	39.7 ± 4.3
VSS (g/L)	123.8 ± 2.4	9.8 ± 0.9	36.2 ± 1.4
TCOD (g/L)	130.0 ± 6.4	14.0 ± 1.1	40.0 ± 2.7
Carbohydrate (gCOD/L)	88.6 ± 3.3	1.3 ± 0.6	22.9 ± 2.0
Ammonia (mg/L)	19.7 ± 2.6	14.2 ± 1.4	7.5 ± 2.8
TKN (g/L)	1.6 ± 0.2	0.9 ± 0.1	0.6 ± 0.2

[a] FW and WAS were mixed at a volatile suspended solid (VSS) mass ratio of 6:1. Then, given tap water was added to dilute the mixture.

Table 2

Experimental ranges and levels of independent factors for RSM study

Factors	Symbols	Units	Coded levels of factors				
Salt dosage	A	g/L	0	10	20	30	40
Fermentation time	B	d	1	2	3	4	5

Table 3

Alpha-diversity analysis of the Blank reactor, R-10, and R-30.

	Blank (3d)	Blank (7d)	R-10 (3d)	R-10 (7d)	R-30 (3d)	R-30 (7d)
Chao 1[a]	965	1498	1158	1264	919	1238
Ace[b]	1008	1558	1241	1272	919	1332
Shannon[c]	6.97	8.02	6.41	7.64	5.06	6.23
Simpson[d]	0.97	0.99	0.95	0.98	0.80	0.93

Values in parentheses are fermentation time

[a] Chao1 richness index: A higher number indicates the higher richness.

[b] ACE richness index: A higher number represents the higher richness

[c] Shannon diversity index: A higher value represents higher diversity (being sensitive to the richness and the few OTUs).

[d] Simpson richness index: A higher number indicates higher diversity (being sensitive to the evenness and the dominant OUT).

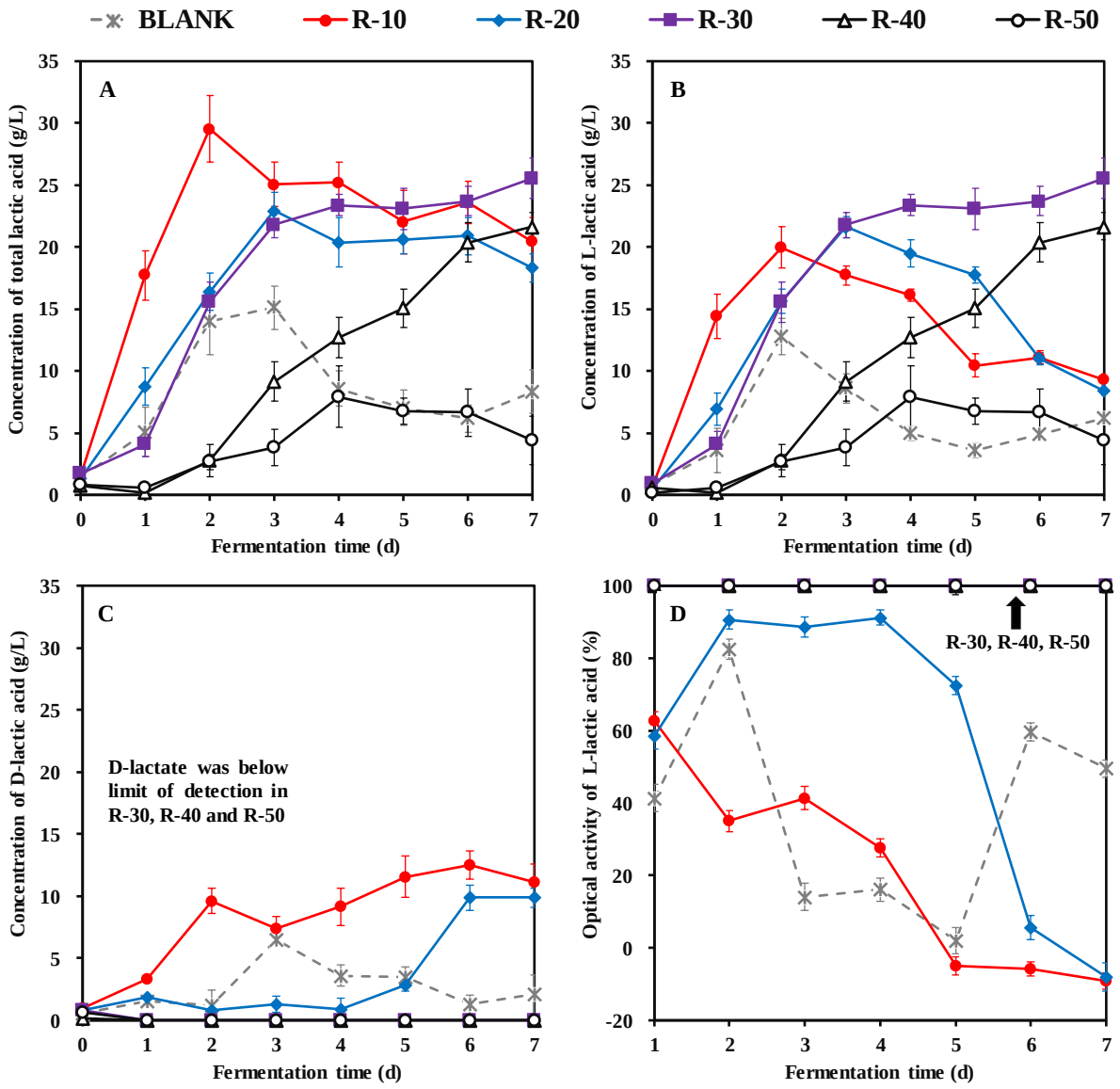

Fig.1. Impact of salinity in FW on the production of total lactic acid (A), L-lactic acid (B), D-lactic acid (C), and optical activity of L-lactic acid (D).

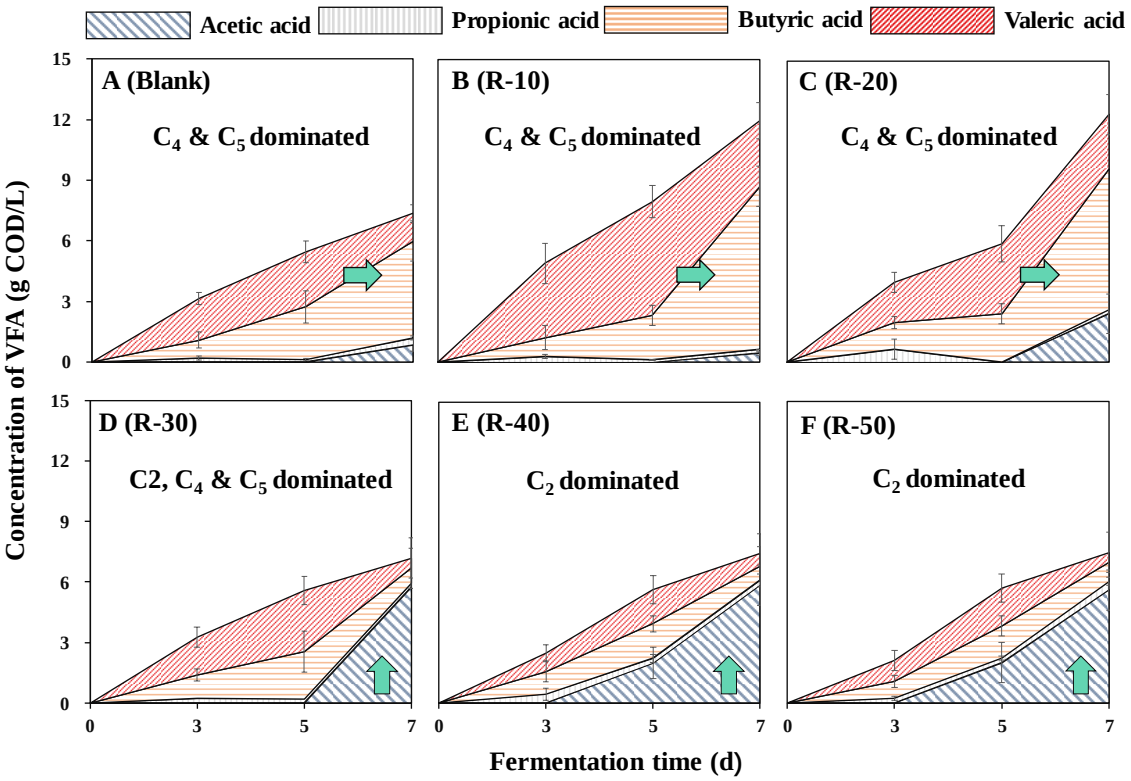

Fig. 2. Effects of salt concentration on the VFA production and composition. (Salt concentration from 0 to 50 g/L (A-F)).

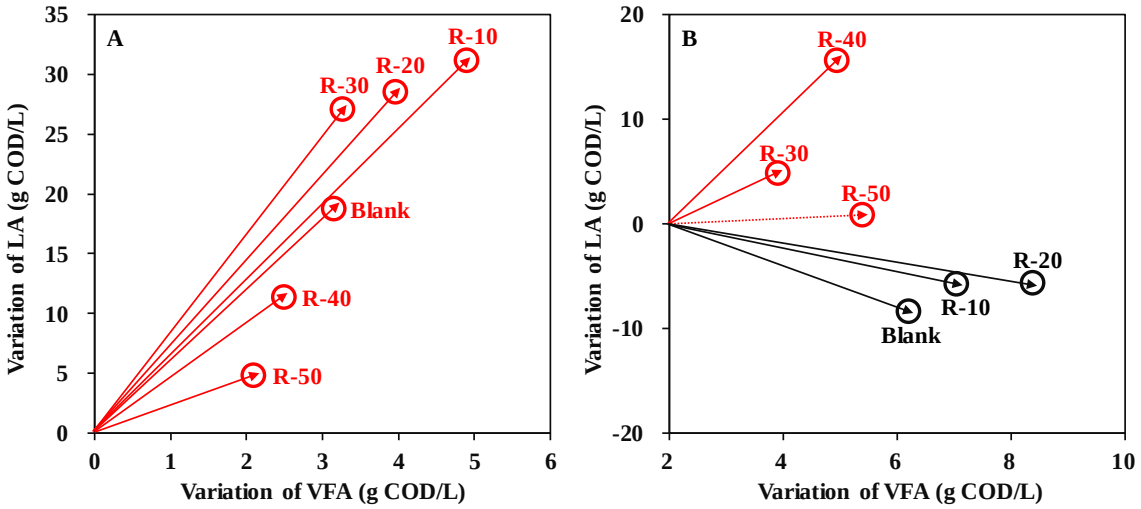

Fig. 3. Correlation between incremental production of LA and VFA during day 0 to 3 (A) and day 3 to 7 (B). (Lines with red mean positive correlation (between variations of LA and VFA) while black means negative correlation).

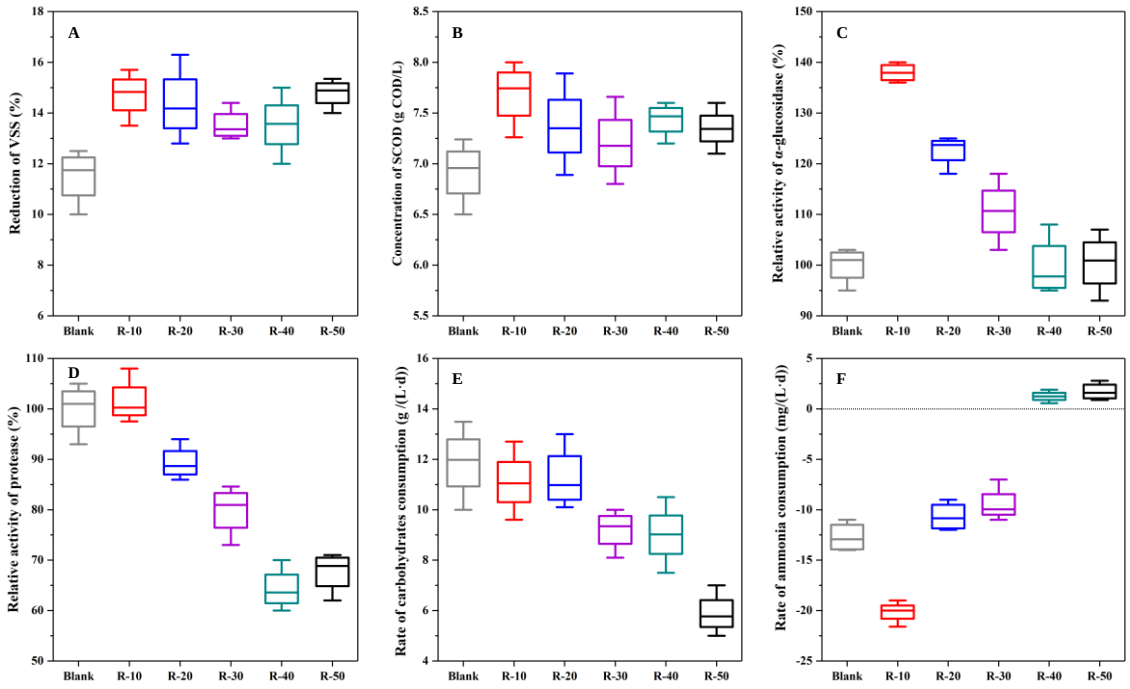

Fig. 4. Impact of salinity on solubilization, hydrolysis, glycolysis during fermentation from 0 (blank) to 50 g/L (R-50). Reduction of VSS on day 1 (A); concentration of SCOD on day 1(B); The relative activity of α-glucosidase on day 3 (C); The relative activity of protease on day 3 (D); The rate of carbohydrate consumption (glycolysis) from day 1 to day 2 (E); The rate of ammonia consumption from day 0 to day 3 (F).

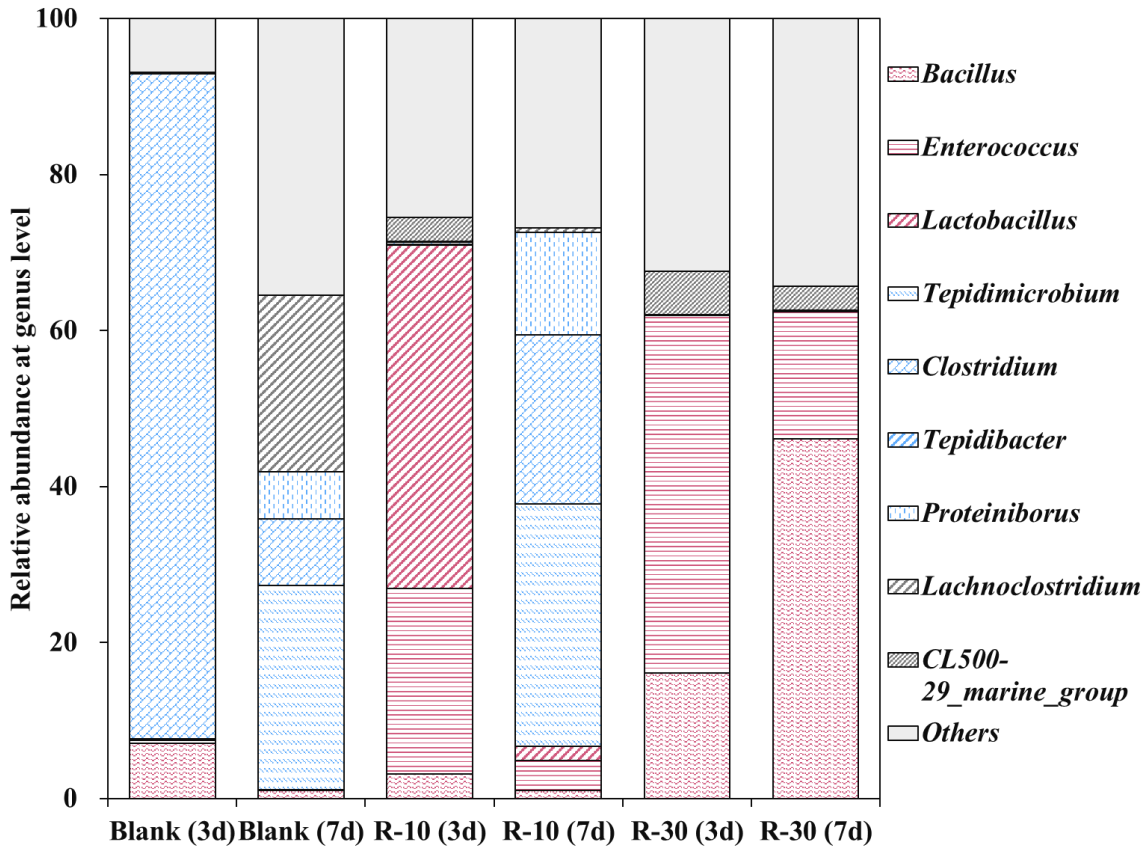

Fig. 5. Microbial community shift at the genus level in the blank reactor, R-10, and R-30 (red for LAB and blue for VFA producers).

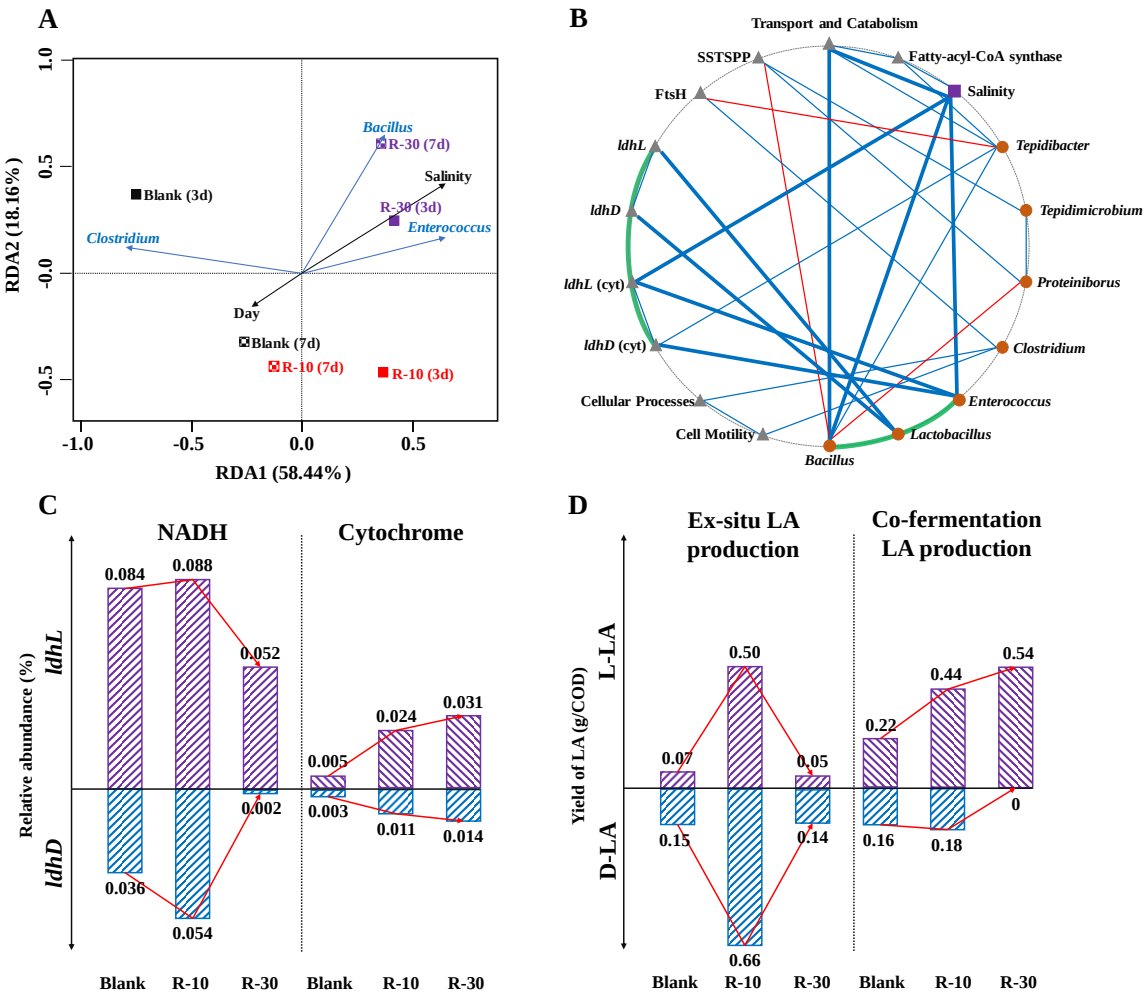

Fig.6. Correlation analysis among microbial communities, KEGG predicted functional gene, and operational parameter. Correlation between the microbial community and environmental factors (salinity and fermentation time) by RDA (A); network analysis revealing the co-occurrence patterns between KEGG predicted functional gene, microbial taxa, and salinity (B). (A connection represents a strong (Spearman's correlation coefficient $R^2 > 0.8$) and significant (P-value <0.05) correlation. Blue and red lines mean positive and negative correlations, respectively. Circles represent microbial taxa, triangles represent KEGG predicted functional gene, and square represents salinity). Variation of the relative abundances of LA related genes, including *ldhL*, *ldhD*, *ldhL* (cytochrome), and *ldhD* (cytochrome) (C), and comparison of LA production ex-situ and in co-fermentation (D). (Red lines represent the variation tendency)